CHIN. PHYS. LETT. Vol. 32, No. 11 (2015) 117304

Miniband Formation in GaN/AlN Constant-Total-Effective-Radius Multi-shell Quantum Dots *

Solaimani M.**

Department of Physics, Qom University of technology, Qom, Iran

(Received 31 May 2015)

We study the procedure of miniband formation in GaN/AlN constant-total-effective-radius multi-shell quantum dots (CTER-MSQDs) by calculating the subband energies. We find a different behavior of the miniband widths and miniband gaps when the number of wells changes. It is shown that with increasing the inner quantum dot radius $R_{\rm in}$, the number of minigaps decreases; with increasing the outer quantum dot radius $R_{\rm out}$, the number of minigaps increases. We show that in the CTER-MSQDs systems, two kinds of minigaps exist: in the type (i) ones, minigaps increase monotonically when the number of wells increases while in the type (ii) ones, with increasing the number of wells, some of minigaps create, increase, at a critical number of wells decrease and finally vanish. Thus tuning of the minigaps and miniband widths in the CTER-MSQDs systems by using the number of wells, inner and outer quantum dot radii $R_{\rm in}$ and $R_{\rm out}$ is now possible.

PACS: 73.21.Cd DOI: 10.1088/0256-307X/32/11/117304

Minibands are one of the most important characteristics of the superlattices. Studies of the miniband formation procedures are suitable to calculate some physical properties which have an essential role in the semiconductor quantum devices such as THz detectors,[1] quantum cascade detectors,[2] Bloch oscillators and quantum cascade lasers.[3] In the literature, electronic transport is one of the most important properties of superlattices. Miniband formation has also been an important research field during the last few decades.[4,5] In the theory of minibands, different scopes such as miniband transport phenomena[6,7] and collapse of the minibands[8,9] have been investigated. In these studies, both wide[10] and narrow[11] miniband forms have been explored.

Among the commonly employed theoretical tools, studying electronic properties of semiconductor quantum structures is the envelope function method which for example can be used in determining transmission coefficients, bound state energies, or the behavior under the effect of electric and magnetic fields.[12–20] In this framework, the effective mass approximation is usually considered. This is due to the fact that the potential structures generated are usually near the bottom of the conduction band of the barrier and well material. In the standard model the potential wells and barriers are rectangular. This is due to the abrupt jump of the potential energy between successive materials.

Shapes and arrangements of the building blocks severely affect the miniband formation scenario. In the literature, Fibonacci[21] and Pascal-type[22] superlattices and also the effect of the barrier widths on the miniband formation and miniband widths have been extensively investigated before.[23,24]

Spherical quantum dots are of special importance. Changing the number of wells along the radius in a quantum dot can affect the different properties of the system such as electronic[25] and optical properties.[25,26] In this situation, we have a quantum-dot quantum well system. However, the superlattice form of multi-layer quantum dots with fixed radius has not yet been studied.

Here we have used another interesting way which we expect may find a good situation in the modern technologies. Retaining the total length of the structure constant and varying the number of wells within it in our recent studies,[27–30] led to constant total effective length multiple quantum wells (CTEL-MQWs), constant total effective radius multi-well quantum rings (CTER-MWQRs). We expect that our method of building blocks can lead to smaller nano-devices with optimized physical properties. In the current work, we have studied the miniband formation procedure in CTER-MSQDs. This is carried out through direct numerical calculation (a finite difference method) of the subband energies. Finally we note that the experimental fabrication of such semiconductor quantum structures is also possible.[31–35]

Behavior of electrons in quantum dots can be described by means of the radial part of the spherical Schrödinger equation within the effective mass approximation

$$\Big[-\frac{\hbar^2}{2m^*}\Big(\frac{\partial^2}{\partial r^2}+\frac{2}{r}\frac{\partial}{\partial r}-\frac{L(L+1)}{r^2}\Big) + V(r)\Big]\psi(r)=E\psi(r), \tag{1}$$

where m^* is the effective mass, and $V(r)$ is the geometrical confinement potential which we have defined as

$$V(r)=\begin{cases}V_{\rm conf}, & N=1,3,\ldots\\ 0, & N=2,4,\ldots\end{cases}$$

$$\frac{i-1}{2N+1}R_{\rm in}<r<\frac{i}{2N+1}R_{\rm out} \tag{2}$$

*Supported by the Iranian Nanotechnology Initiative Council, and the Shahrood University of Technology.

**Corresponding author. Email: solaimani@qut.ac.ir

© 2015 Chinese Physical Society and IOP Publishing Ltd

where N is the number of wells, L is the orbital quantum number, $V_{\rm conf}$ is the constant relative conduction band offset, i shows the ith well or barrier, and $R_{\rm in}$ and $R_{\rm out}$ are the inner and outer quantum dot shell radii, respectively. For illustration purposes, a schematic diagram for a typical single-well quantum dot is presented in Fig. 1. We have used the finite difference method[36] to solve Eq. (1) and to calculate the subband energies.

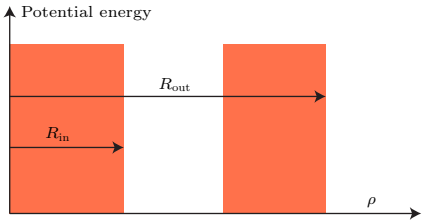


Fig. 1. Schematic representation of a typical single well-quantum dot system. Here we have depicted the potential profile versus radius r.

In this work, we have studied GaN/AlN CTER-MSQDs systems. The values of the effective masses $m^* = 0.12m_{\rm e}$ for GaN, and $m^* = 0.48m_{\rm e}$ for AlN[37] and 1.28 eV confinement potential[37] assumed. To determine the effect of the size of the quantum dot, we have selected different outer radii of quantum dots, i.e., 400, 600 and 1000 Å.

By using the finite difference method we have solved Eq. (1) and calculated the subband energies. When we plot these subband energies as a function of the number of wells in the quantum dot we have found Figs. 2–4. In some of these figures we have only plotted the subband energies for $L = 0$ (specified on the figurer) while in Figs. 3(a) and 4(a) we compared the result for $L = 0$, 1 and 2. This is due to the fact that there is not new physics in the systems with larger L and thus we have only presented the diagram corresponding to $L = 0$. In all of Figs. 2–4 we have assumed that $R_{\rm out}$ is constant (400, 600 and 1000 AA) and then we have changed the number of wells within these constant $R_{\rm out}$. Meanwhile, we have supposed that all of the wells and barriers in a system have the same thickness (e.g., in 3-well CTER-MSQDs we have 3 wells and 4 barriers which have the same thickness). By increasing the number of wells at fixed $R_{\rm out}$, each well and barrier thickness will be reduced. Reduction of the barrier thickness leads to tunneling of the electrons between adjacent wells and thus gradually a superlattice will be created. In this situation, minibands will be formed and since the number of degenerate states in a subband energy of a multiple quantum well system is equal to the number of wells in that system, a superlattice which is created from systems with larger number of wells has wider minibands. This is just the phenomena we observe in the Figs. 2–4, i.e., the miniband width increases when the number of wells increases. Finally, the maximum number of wells in each system is selected based on the fact that there are some technological limitations on making barriers or wells with very small thicknesses. We are not allowed experimentally to further increase the number of wells.

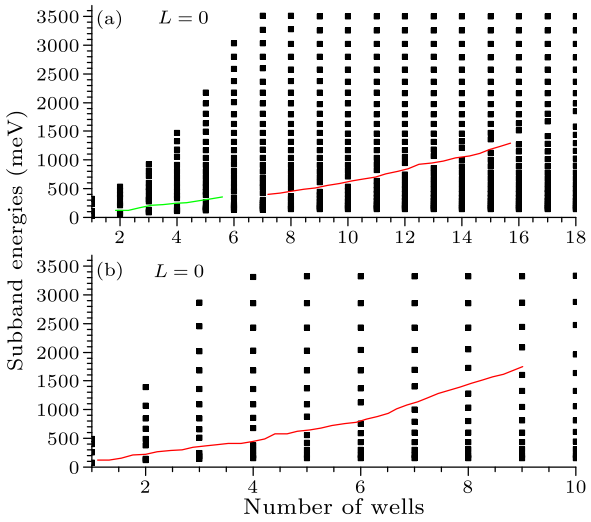


Fig. 2. Variation of the subband energies as a function of the number of wells for CTER-MSQDs with $R_{\rm out} = 400$ Å. Two different $R_{\rm in} = 0$ and $R_{\rm in} = 200$ Å are presented in (a) and (b), respectively. First and second mini-gaps are shown by red and green lines, respectively.

Now, we study the effect of $R_{\rm in}$ and $R_{\rm out}$ in CTER-MSQDs systems on minibands and minigaps. In Fig. 4(a), we have selected $R_{\rm in} = 0$ and $R_{\rm out} = 400$ Å. Here red and green lines show the first and second minigaps, respectively. Both of these lines monotonically increase when the number of wells increases. This is not the behavior we usually see in the usual superlattices. As we know from the quantum mechanics, when the well width decreases the value of the discrete energy levels increases (e.g., the ground state energy takes a larger value when the well width increases). Here when we increase the number of wells in a fixed quantum dot radius, the width of each quantum well also decreases. Thus when we increase the number of wells, the minibands and minigaps start to be created and these energies find larger values since the well width has been decreased. Thus the main reason for this monotonic increasing behavior is the decrease of the well widths when the number of well increases. Figure 5 shows the first three minibands of a superlattice with 1 nm thickness of each well and barrier. Variation of the first and second minigaps as a function of the number of wells in Figs. 2–4 is not monotonic. For example, the first minigap (indicated by the red line in Fig. 2(a)) increases monotonically when the number of wells increases while the second minigap (indicated by the green line) increases from single to four-wells CTER-MSQDs and then by further increasing the number of wells decreases. As we know from the basic quantum mechanics, the spacing of the energy levels increases by the index of a state (e.g., $(E_3 - E_2) > (E_2 - E_1)$, where E_i is ith energy level). This is just what we observe in our diagrams. However with the increase of $R_{\rm in}$ the spacing grows larger (e.g., compare Fig. 2(a) with Fig. 2(b)). A difference between Figs. 2(a) and 2(b) is that we have

two minigaps in Figs. 2(a) and a minigap in Figs. 2(b). If we see Figs. 2–4, we conclude that with increasing $R_{\rm in}$ the number of minigaps decreases. Comparison of Figs. 2(a), 3(a) and 4(a) also reveals that with increasing $R_{\rm out}$ the number of minigaps increases. A common fact in Figs. 2–4 is that we have two kinds on minigaps: (i) some of the minigaps increase monotonically when the number of wells increases. The first minigaps (red lines) are of this kind. (ii) By increasing the number of wells some of the minigaps create, increase, at a critical number of wells decrease and finally vanish. The second minigaps (green lines) are of this kind. Colored lines indicate the position of the minigaps in the plane of subband energy-number of wells. Higher minigaps in a typical system within all of Figs. 2–4 have a higher slope. Minigaps in systems with larger orbital quantum number L also have a higher slope (e.g., compare panels A, B and C of Fig. 3(a)). The final fact is that by using the number of wells, inner and outer quantum dot radii $R_{\rm in}$ and $R_{\rm out}$, we are able to tune the minigaps and miniband widths in the CTER-MSQD systems.

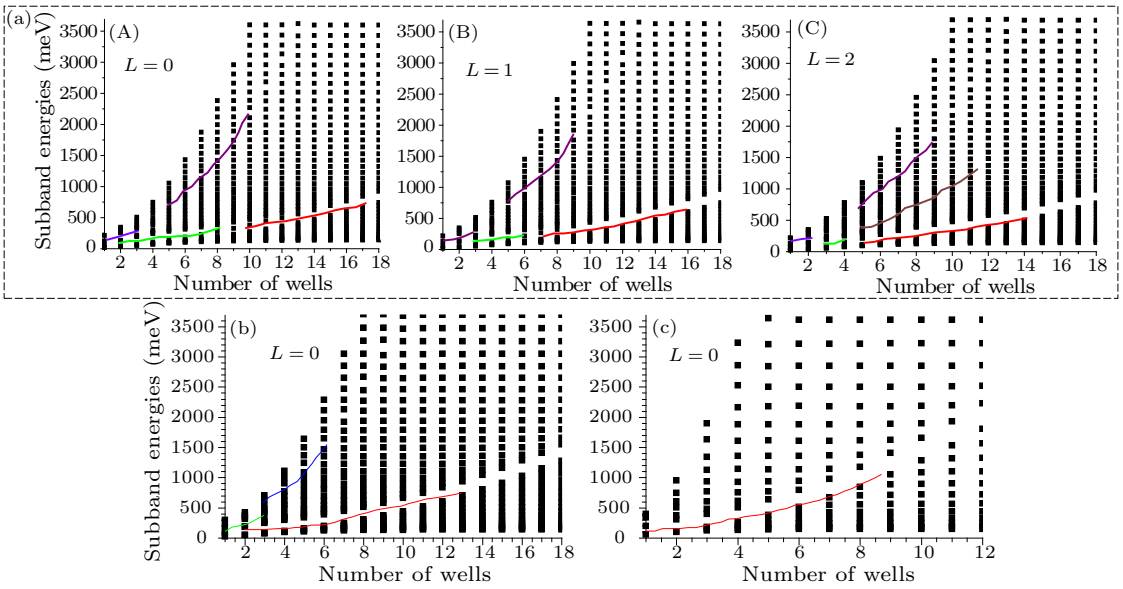


Fig. 3. Variation of the subband energies as a function of the number of wells for CTER-MSQDs with $R_{\rm out} = 600$ Å. Three different $R_{\rm in} = 0$, 150 and 350 Å are presented in (a)–(c), respectively. The first–fifth mini-gaps are shown by red, green, violet, brown and purple lines, respectively. In (a), the results for $L = 0$, 1 and 2 are compared.

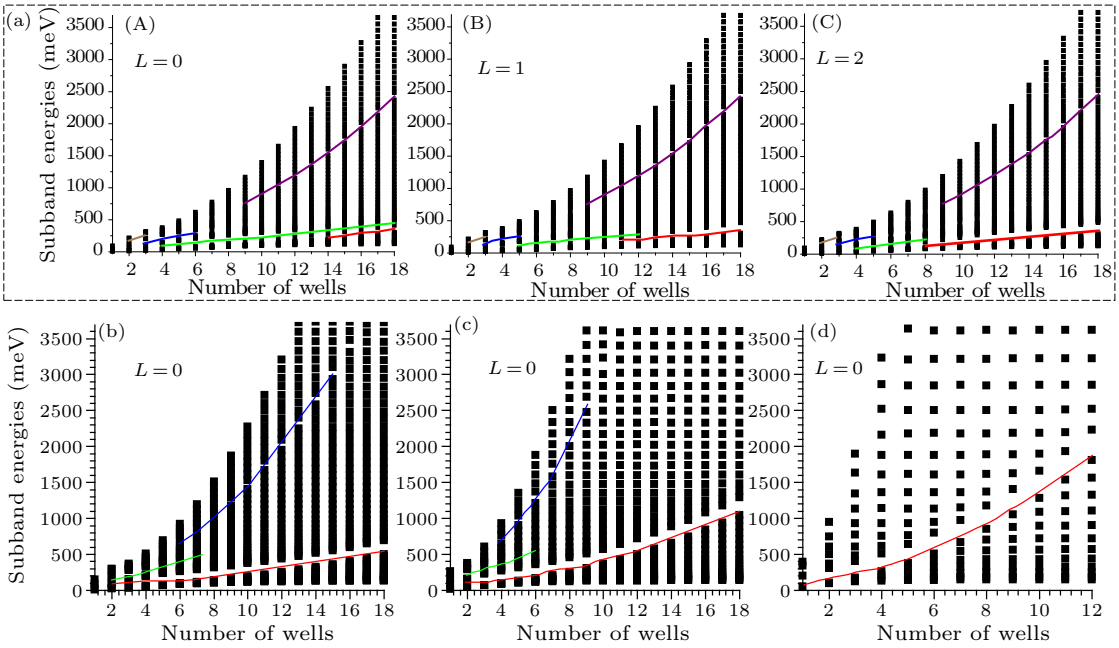


Fig. 4. Variation of the subband energies as a function of the number of wells for CTER-MSQDs with $R_{\rm out} = 1000$ Å. Four different $R_{\rm in} = 0$, 250, 500 and 750 Åare presented in (a)–(d), respectively. The first–fifth mini-gaps are shown by red, green, violet, brown and purple lines, respectively. In (a), the results for $L = 0$, 1 and 2 are compared.

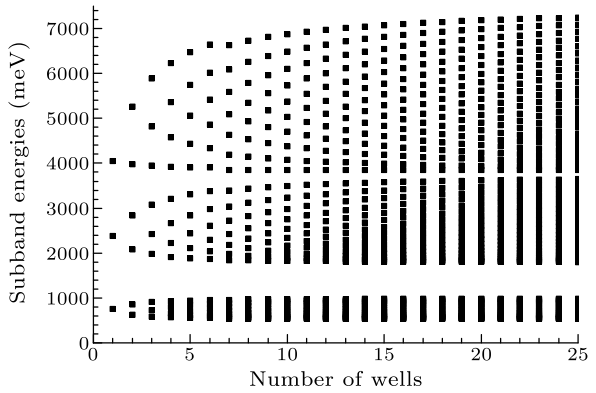


Fig. 5. The first three minibands of a constant total effective length-multiple quantum well system (CTEL-MQWs) with 1 nm thickness of each well and barrier.

In summary, the miniband formation procedure in GaN/AlN constant total effective radius multi-shell quantum dots has been investigated by subband energy calculations. We observe that: (1) with increasing $R_{\rm in}$ the number of minigaps decreases, (2) with increasing $R_{\rm out}$ the number of minigaps increases, and (3) we have two kinds of minigaps: type (i) some of the minigaps increase monotonically when the number of wells increases. Type (ii) with increasing the number of wells some of the minigaps create, increase, at a critical number of wells decrease and finally vanish. Thus by using the number of wells, inner and outer quantum dot radii $R_{\rm in}$ and $R_{\rm out}$, we are able to tune the minigaps and miniband widths in the CTER-MSQD systems.

References

[1] Klappenberger F, Ignatov A A, Winnerl S, Schomburg E, Wegscheider W and Renk K F 2001 *Appl. Phys. Lett.* **78** 1674

[2] Giorgetta F R, Baumann E, Graf M, Ajili L, Hoyler N, Giovannini M, Faist J and Hofstetter D, Krötz P and Sonnabend G 2007 *Appl. Phys. Lett.* **90** 231111

[3] Willenberg H, Dohler G H and Faist J 2003 *Phys. Rev.* B **67** 085315

[4] Klos J W and Krawczyk M 2008 *Materials Science-Poland* **26** 965

[5] Behn U, Linder N, Grahn H T and Ploog K 1995 *Phys. Rev.* B **51** 17271

[6] Pusep Y A, Chiquito A J, Mergulhao S and Galzerani J C 1997 *Phys. Rev.* B **56** 3892

[7] Hyldgaard P and Jauho A P 1990 *J. Phys.: Condens. Matter* **2** 8725

[8] Holthaus M 1992 *Phys. Rev. Lett.* **69** 351

[9] Zhao X G 1997 *Phys. Lett.* A **230** 229

[10] Shimada Y, Hirakawa K and Lee S W 2002 *Appl. Phys. Lett.* **81** 1642

[11] Grahn H T, Klitzing K V Ploog K and Dohler G H 1991 *Phys. Rev.* B **43** 12094

[12] Cota E, Jose J V and Monsivais G 1987 *Phys. Rev.* B **35** 8929

[13] Lunz U, Keim M, Reuscher G, Fischer F, Schull K, Waag A and Landwehr G 1996 *J. Appl. Phys.* **80** 6329

[14] Carpena P, Gasparian V and Ortuno M 1997 *Z. Phys.* B **102** 425

[15] Chen S D, Narayan C and Karakashian A S 1996 *Physica* B **228** 239

[16] Ferreira R and Bastard G 1997 *Rep. Prog. Phys.* **60** 345

[17] Zhu J X, Wang Z D and Gong C D 1996 *J. Appl. Phys.* **80** 2291

[18] Carpena P 1997 *Phys. Lett.* A **231** 439

[19] Bouchard A M and Luban M 1995 *Phys. Rev.* B **52** 5105

[20] Zekri N, Schreiber M, Ouasti R, Bouamrane R and Brezini A 1995 *Z. Phys.* B **99** 381

[21] Cai X B and Xuan X F 2004 *Opt. Commun.* **240** 227

[22] Saldana X I, Contreras-Solorio D A and Lopez-Cruz E 2007 *Revista Mex. Física* **53** 310

[23] Ferry D K, Goodnick S M and Bird J 2009 *Transport in Nanostructures* (Cambridge: Cambridge University Press) 2nd edn chap 2 p 40

[24] Harrison P 2005 *Quantum Wells, Wires and Dots, Theoretical and Computational Physics of Semiconductor Nanostructures* 2nd edn (New York: John Wiley & Sons) chap 2 p 55

[25] Chang K 2000 *Phys. Rev.* B **61** 4743

[26] Chang K and Xia J B 1998 *Phys. Rev.* B **57** 9780

[27] Solaimani M, Izadifard M, Arabshahi H and Sarkardei M R 2013 *J. Lumin.* **134** 699

[28] Solaimani M, Izadifard M, Arabshahi H and Sarkardei M R 2013 *J. Lumin.* **134** 88

[29] Solaimani M 2014 *Solid State Commun.* **200** 66

[30] Solaimani M, Lavaei L and Ghalandari M 2015 *Superlattices Microstruct.* **82** 1

[31] Widmann F, Daudin B, Feuillet G, Samson Y, Rouviere J L and Pelekanos N 1998 *J. Appl. Phys.* **83** 7618

[32] Moumanis K, Helman A, Fossard F, Tchernycheva M, Lusson A and Julien F H, Damilano B, Grandjean N and Massies J 2003 *Appl. Phys. Lett.* **82** 869

[33] Songmuang R, Kalita D, Sinha P, Hertog M, André R, Ben T, González D, Mariette H and Monroy E 2011 *Appl. Phys. Lett.* **99** 141914

[34] Lv W, Wang L, Wang J, Hao Z and Luo Y 2012 *Nanoscale Res. Lett.* **7** 617

[35] Lv W, Wang, Wang J, Xing Y, Zheng J, Yang D, Hao Z and Luo Y 2013 *Jpn. J. Appl. Phys.* **52** 08JG13

[36] Chari M V K and Salon S J 2000 *Numerical Methods in Electromagnetism* (New York: Academic Press) chap 2 p 80

[37] Vurgaftman I Meyer J R and Ram-Mohan L R 2001 *J. Appl. Phys.* **89** 5815